Removal of impurities from metallurgical grade silicon by electron beam melting*

Luo Dawei(罗大伟)[1,†], Liu Ning(刘宁)[1], Lu Yiping(卢一平)[1], Zhang Guoliang(张国梁)[1], and Li Tingju(李廷举)[1,2,†]

[1]School of Materials Science and Engineering, Dalian University of Technology, Dalian 116024, China
[2]Ministry of Education Key Laboratory of Materials Modification by Laser, Ion and Electron Beams, Dalian University of Technology, Dalian 116024, China

Abstract: Solar cells are currently fabricated from a variety of silicon-based materials. Now the major silicon material for solar cells is the scrap of electronic grade silicon (EG-Si). But in the current market it is difficult to secure a steady supply of this material. Therefore, alternative production processes are needed to increase the feedstock. In this paper, EBM is used to purify silicon. MG-Si particles after leaching with an initial purity of 99.88% in mass as starting materials were used. The final purity of the silicon disk obtained after EBM was above 99.995% in mass. This result demonstrates that EBM can effectively remove impurities from silicon. This paper mainly studies the impurity distribution in the silicon disk after EBM.

Key words: silicon refining; electron beam melting; metallurgical grade silicon; solar grade silicon
DOI: 10.1088/1674-4926/32/3/033003 **EEACC:** 2520C

1. Introduction

The global PV industry has been developing rapidly over the past decade, which has led to a large demand for silicon materials. Silicon is divided into four categories according to its purity: metallurgical grade silicon (MG-Si), chemical grade silicon (CG-Si), solar grade silicon (SOG-Si) and electronic grade silicon (EG-Si). Off-spec scrap silicon from the semiconductor industry is used for solar cells but in the current market it is difficult to secure a steady supply of this material. Therefore, development of a process to produce silicon at low cost is definitely necessary. Production of high purity silicon by EBM processes has been developed extensively[1−3].

A number of studies have illustrated the technical viability of the EBM process with excellent results in terms of the final purity of silicon. Pires *et al*.[4] purified MG-Si with an initial purity of 99.91% in mass and a weight of 280 g as starting materials by EBM, and obtained a silicon sample with purity of 99.999% eventually. Takashi *et al*.[5] found that 90% carbon, 75% aluminum, 89% calcium and 93% phosphorus were removed by EBM treatment under 10^{-2} Pa for 30 min. A first order rate equation was used for the removal of carbon, calcium and aluminum, and a second order equation fit for the dephosphorization. Kazuhiro *et al*.[6, 7] carried out industrial scale experiments for an EBM purification process. MG-Si with 25 ppmw of phosphorus was successfully purified to below 0.1 ppmw. Sorokin *et al*.[8] showed that the phosphorus content decreased from 0.001% to 0.0003% after EBM under a scanning electron beam in an 8.9×10^{-3} Pa vacuum. Japan's JET Company invented a new technology that used an electron beam and a plasma beam combined with directional solidification to prepare SOG-Si. A silicon ingot with a weight of 100–300 kg and a conversion efficiency of 14.1% was successfully produced[9]. The above studies demonstrate that the EBM has been studied extensively and in depth in other countries, but research on the preparation of SOG-Si by EBM is still at its initial stages in China for various reasons.

This paper presents a new method of purification that combines EBM and a directional solidification process. EBM as an important part of the purification process should be analyzed and researched in detail. The purpose of this paper is to carry out a preliminary study of the preparation of SOG-Si by EBM. The content and distribution of impurities in the sample are studied after EBM. The electron probe microanalysis (EPMA) of impurities at different locations in a silicon disk is also discussed.

2. Experimental procedures

A schematic diagram of the structure and principle of EBM is shown in Fig. 1. Silicon particles were washed with acetone in an ultrasound cleaner with the objective of removing possible solid residues from the surface before EBM and 400 g silicon was placed inside the copper crucible for each experiment. Silicon was heated with the gradual elevation of the electron beam power until the whole of the silicon was melted and then the power was kept at a constant value for a certain time. After refining, the power was slowly reduced until the beam disappeared in the center of the sample, which provided a temperature gradient from the border to the center of the sample that favored the segregation of impurities. The process parameters are indicated in Table 1. The impurity contents and surface analysis were confirmed by inductively coupled plasma mass spectrometry (ICP-MS) and scanning electronic microscopy (SEM).

* Project supported by the National Natural Science Foundation of China (No. 50674018).
† Corresponding author. Email: luodlut@yahoo.com.cn; tjuli@dlut.edu.cn
Received 30 August 2010, revised manuscript received 15 October 2010

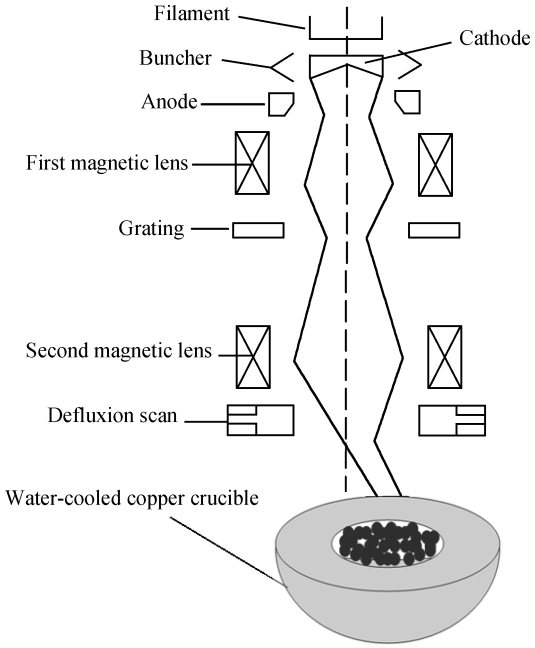

Fig. 1. Schematic diagram of the structure and principle of an electron beam furnace.

Table 1. Experimental parameters used in electron beam melting.

Parameter	Value
Melting time	20 min
Beam power	10–15 kW
Internal pressure of the furnace	2.5×10^{-3} to 5.0×10^{-3} Pa

3. Results and discussion

3.1. Macro-morphology of silicon disk

Figure 2 shows the top and bottom views of the silicon disk obtained after EBM with a diameter of 130 mm and a thickness of 25 mm. The bottom of the silicon disk was very coarse because it made contact with the refrigerated copper crucible, which prevented it from melting fully under EBM. Figure 3 shows a schematic representation of the regions of the silicon disk for impurity concentration analysis.

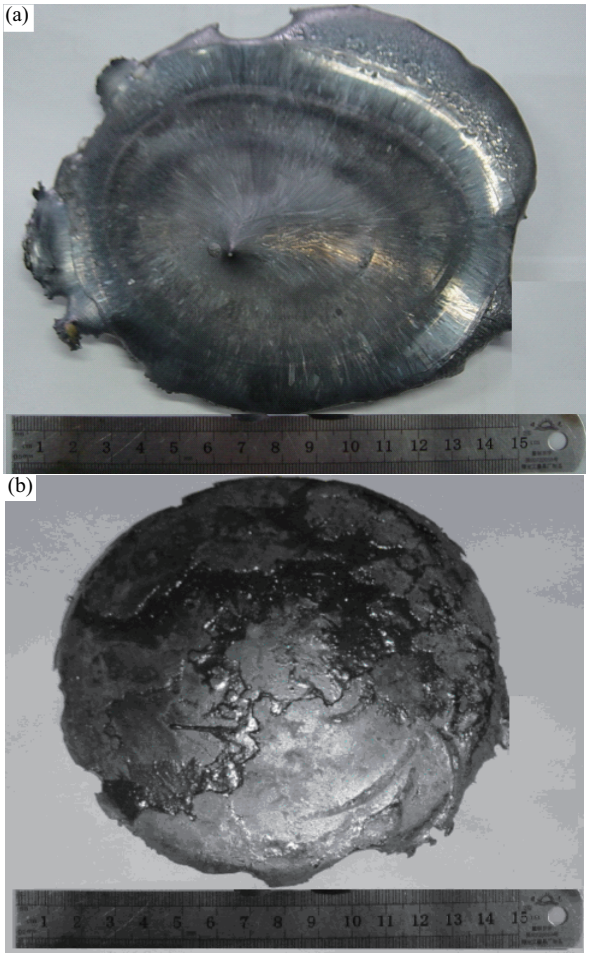

Fig. 2. (a) Top view and (b) bottom view of silicon disk after electron beam melting.

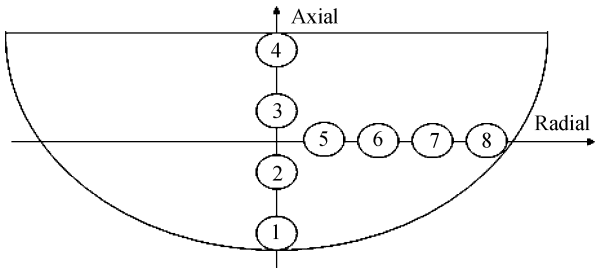

Fig. 3. Schematic representation of the regions of the silicon disk for impurity profile analysis.

3.2. Impurity distribution

3.2.1. Distribution of impurity elements along axial

The distribution of metal impurities and nonmetal elements along the axial are shown in Figs. 4 and 5, respectively. It should be noted that metal elements were dragged from the bottom to the top following the direction of solidification. There was no effect on the distribution of nonmetal elements. The lowest impurity content location was at a height of about 10 mm along the sample thickness. The metal impurity segregation to the top can be explained by their low segregation coefficients. Metal impurities will be pushed into the liquid region during solidification because the effective segregation coefficient of the metal impurities in silicon is much less than unity. Therefore, the content of metal impurities was gradually increased as the ingot height increased.

Figure 6 shows a diagram of the silicon cake solidification process. It can be seen that there were two directions of the temperature gradient during the silicon cake solidification process due to the special structure of the water cooled copper crucible at the same time. That is, the axial temperature gradient and the radial temperature gradient. Metal elements such as Cu, Al, Ti and Fe were effectively dragged to the remaining liquid region during solidification because they had very low segregation coefficients. Thereby, the solidified part was purified. However, directional solidification had little effect on the nonmetal elements, such as C, O, B and P, because these elements had a segregation coefficient close to unity[10]. One noteworthy fact in Fig. 4 is that impurity concentrations at the

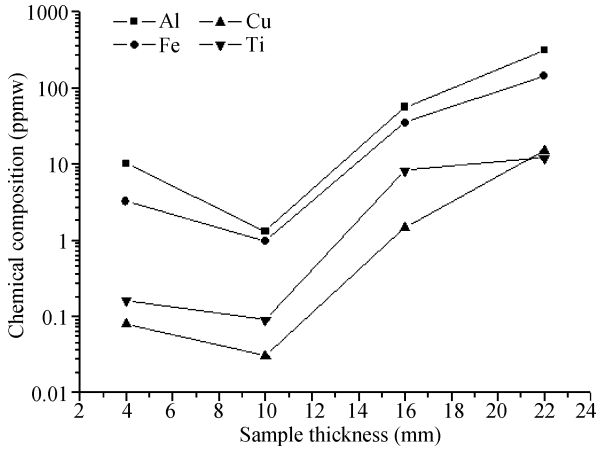

Fig. 4. Distribution of metal impurity elements along axial.

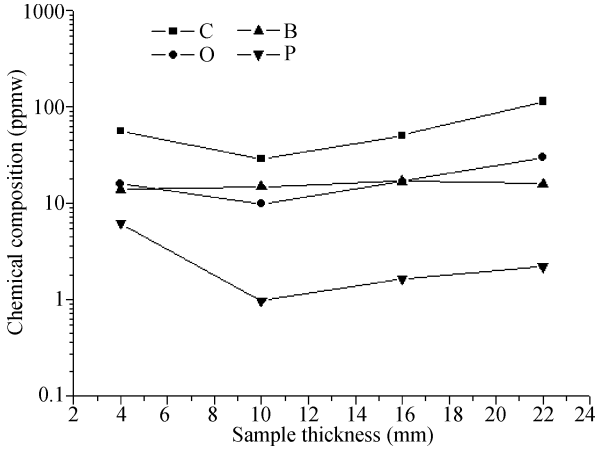

Fig. 5. Distribution of nonmetal impurity elements along axial.

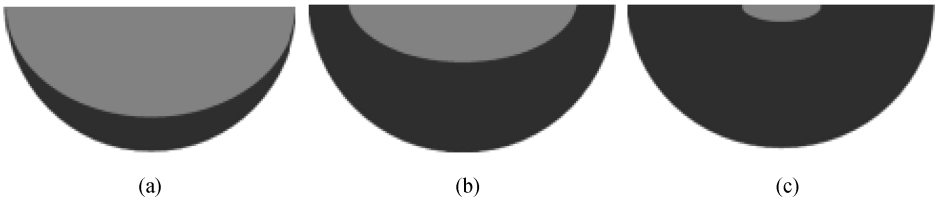

Fig. 6. Schematic diagram of the solidification process of the silicon cake. (a) The initial stage. (b) The intermediate stage. (c) The end stage.

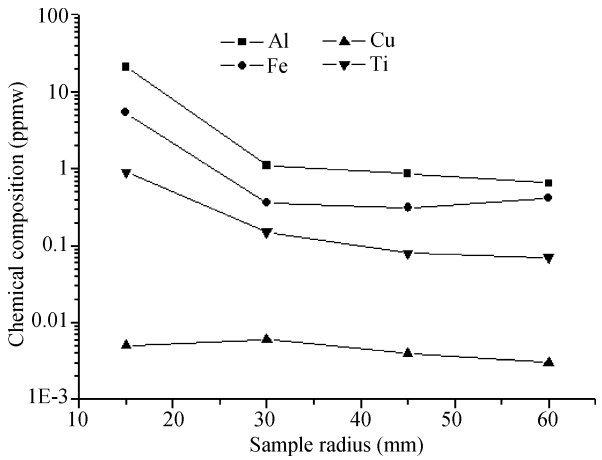

Fig. 7. Distribution of metal impurity elements along sample radial.

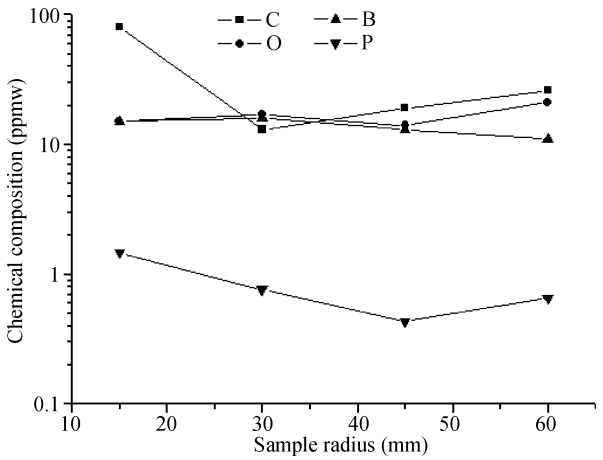

Fig. 8. Distribution of nonmetal impurity elements along sample radial.

bottom present greater than the area just over it. The bottom of the silicon disk solidified before the metallic impurities had enough time to diffuse fully.

3.2.2. Distribution of impurity elements along sample radial

The distribution of impurity elements along the sample radial are shown in Figs.7 and 8. Metal impurities were also dragged from the edge to the center. The effect of directional solidification on the metal impurities still occurred from the edge to the center of the silicon disk due to the temperature gradient. There was almost no change in the nonmetal impurity contents from the edge to the center of the silicon disk. We also found that the C element presented the same distribution trends in Figs. 5 and 8. Carbon could reverse diffusion and be dragged in the opposite direction of solidification because its segregation coefficient is near unity and the atomic radius is smaller than that of silicon[11]. It could also form precipitation and silicon carbides when it was at a high concentration in the polycrystalline silicon.

3.3. Electron microprobe analysis of impurity elements along the axial

In order to understand the distribution of impurity elements in crystalline silicon more clearly, samples were also analyzed by EPMA. Figure 9 shows the electron microprobe analysis of metal elements along the height of the silicon disk.

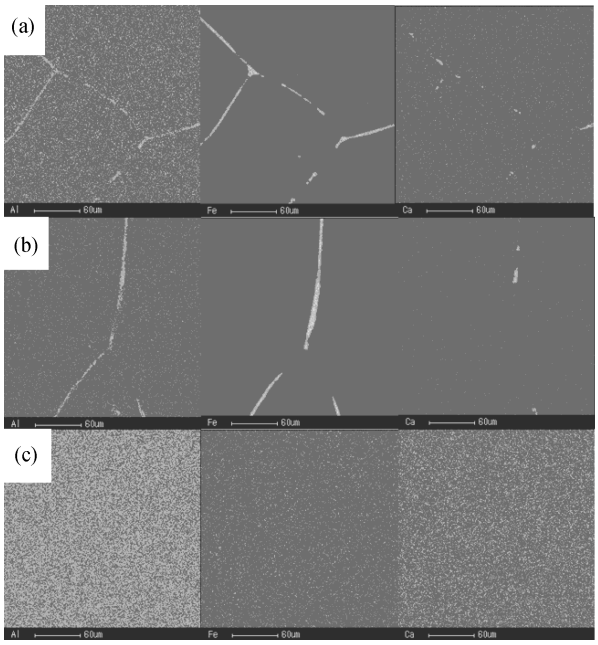

Fig. 9. Electron microprobe analysis of metal impurity elements along the height of the silicon disk. (a) Top of silicon disk. (b) Middle of silicon disk. (c) Bottom of silicon disk.

From Fig. 9(c), we can see that metal elements (Al, Fe and Ca) at the bottom of the silicon disk were distributed very evenly and did not segregate at the grain boundaries because the bottom of the disk was in contact with the refrigerated copper crucible, which led to these metal elements failing to melt fully under EBM .Therefore, they did not have enough time to diffuse. It can be seen from Fig. 9(b) that metal impurities segregated obviously at the grain boundaries in the solidification process. Meanwhile, the number of grain boundaries was relatively small because the grain size was comparatively large. Figure 9(a) shows that most of the inclusions aggregated at the top of solidification portion at the final stage of solidification due to segregation effects. At the same time, the grain size decreased and the number of grain boundaries increased due to the effect of the vertical and horizontal temperature gradients. From the EPMA of the samples, it could be seen that most of the metal impurities were distributed at the grain boundary of the silicon crystals due to segregation effects and only a small part was uniformly distributed in grains. The distribution of non-metallic elements (especially B and P) at the different locations of the silicon disk was basically the same; there was no significant difference between the grain boundary and the grain. The above analysis results were the same as the distribution of the metallic and non-metallic elements along the axial and radial of the silicon disk.

3.4. Effect of vapor pressure on impurity removal efficiency

Figures 10 and 11 show the changes in metallic and non-metallic impurities in the silicon after treatment with different process conditions. We used sample 2 in Fig. 3 to represent the impurity content of the silicon cake because the impurity content in this region was lowest. From Figs. 10 and 11, it could be seen that metal impurities in silicon had been greatly

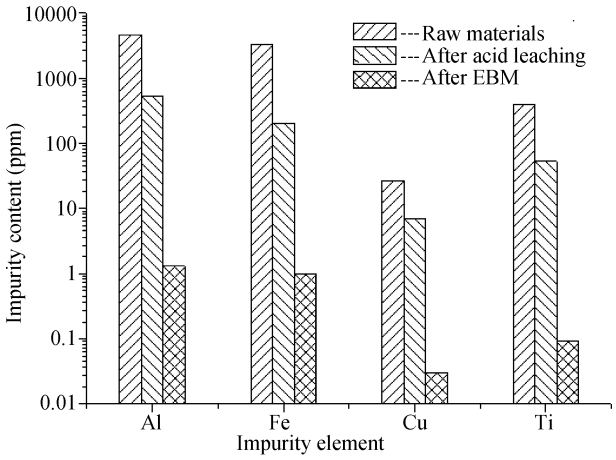

Fig. 10. Changes of metal impurities of after different processes treatments.

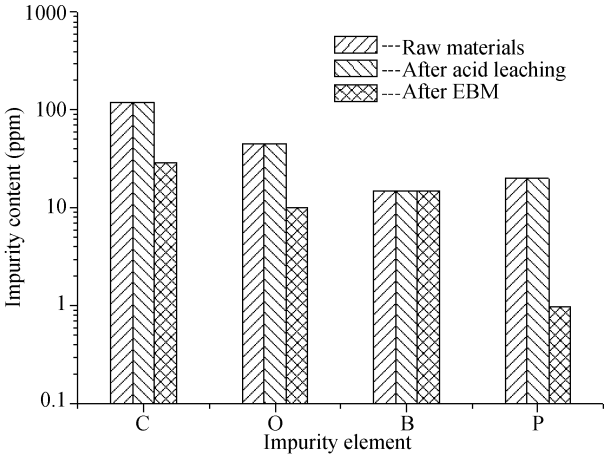

Fig. 11. Changes of non-metallic impurities after different processes treatments.

reduced, while the non-metallic impurities showed no change after leaching treatment. The contents of metal impurities and non-metallic impurities were substantially reduced again after electron beam treatment. There were many kinds of impurity elements in the MG-Si after leaching, but only eight kinds of impurities could be found in the silicon disk after EMB. Because Mn, Mg and Ca have higher vapor pressure than silicon, these elements can be easily removed from silicon through evaporation. Elements such as Ti, Fe, Al and Cu can also be reduced significantly although they have a closer vapor pressure than silicon[12]. However, there was no change in boron contents along the sample axis and radius after electron beam melting. The removal of this element was very difficult because its vapor pressure was very low in relation to that of silicon (10^{-4} Pa for boron and 10^{-1} Pa for silicon). This makes their extraction by vacuum processes difficult. Another difficulty regarding boron extraction was that its segregation coefficient in silicon was near unity, which also made its extraction using a unidirectional solidification process difficult. A process usually used for boron removal was plasma melting in an oxidizing atmosphere (O_2, CO_2 or H_2O). In this process, boron was transformed into the oxide form, increasing its vapor pres-

sure[13].

4. Conclusions

(1) A silicon disk (99.995% in mass) was obtained from MG-Si (99.88% in mass) on the center of the disk after electron beam melting.

(2) The distribution of impurity elements in the silicon disk along the sample axis and radius directions showed different patterns. Metal elements, such as Cu, Al, Ti and Fe, were effectively segregated to the liquid part during solidification because they had very low segregation coefficients. However, directional solidification had little effect on the nonmetal elements, such as C, O, B and P, because these had a segregation coefficient close to unity.

(3) Impurities that had a higher vapor pressure than that of silicon could be easily removed from silicon through evaporation. Elements such as Ti, Fe, Al and Cu could also be reduced significantly, although they had a closer vapor pressure than silicon. The removal of boron was very difficult.

References

[1] Naumov A V. Additional information on the development of solar power and market for silicon raw materials in 2007–2010. Mater Élektron Tekh, 2007, 1: 15

[2] Kazuhiro H Y, Kenkichi S, Yasuhiko K, et al. Solidification and purification of molten silicon. Japanese Patent, No. 08-288219, 1998

[3] Maijer D M, Ikeda T, Cockcroft S L, et al. Mathematical modeling of residual stress formation in electron beam remelting and refining of scrap silicon for the production of solar-grade silicon. Mater Sci Eng, 2005, 390: 188

[4] Pires J C S, Braga A F B, Mei P R. Profile of impurities in polycrystalline silicon samples purified in an electron beam melting furnace. Solar Energy Mater Solar Cells, 2003, 79: 347

[5] Takashi I, Masafumi M. Purification of metallurgical silicon for solar grade silicon by electron beam button melting. ISIJ International, 1992, 32: 635

[6] Kazuhiro H, Noriyoshi Y, Yoshiei K. Evaporation of phosphorus in molten silicon by an electron beam irradiation method. Mater Trans, 2004, 45: 844.

[7] Noriyoshi Y, Kazuhiro H, Yoshiei K. Removal of metal impurities in molten silicon by directional solidification with electron beam heating. Mater Trans, 2004, 45: 850

[8] Osokin V A, Shpak P A, Ishchenko V V, et al. Electron-beam technology for refining polycrystalline silicon to be used in solar power applications. Metallurgist, 2008, 52: 121

[9] Yuge N, Abe M, Hanazawa K, et al. Purification of metallurgical grade silicon up to solar grade. Progress in Photovoltaics: Research and Applications, 2001, 9: 203

[10] Möller H J. Semiconductors for solar cell applications. Progress in Materials Science, 1991, 35: 205

[11] Barbosa L C. Zone refining of silicon. Dissertation, Faculdade de Engenharia de Campinas, Universidade Estadual de Campinas, Campinas, Sao Paulo, Brazil, 1981: 304

[12] Pires J C S, Otubo J, Braga A F B, et al. The purification of metallurgical grade silicon by electron beam melting. Journal of Materials Processing Technology, 2005, 169: 16

[13] Ikeda T, Maeda M. Elimination of boron in molten silicon by reactive rotating plasma arc melting. Mater Trans JIM, 1996, 37: 983